ELSEVIER

Thin Solid Films 322 (1998) 344–345

thin solid films

Author Index of Volume 322

Anderson, A.A. 259
Armand, P. 85
Asai, K. 188

Babelon, P. 63
Banerjee, A. 340
Bellad, S.S. 93
Bernstein, E. 238
Bewilogua, K. 206
Bhosale, C.H. 93
Boffoué, M.O. 132
Boo, J.-H. 9
Bourgeois, S. 63
Bovier, C. 238
Brett, C.M.A. 263
Brunet, F. 143

Carter, G. 177
Cavaleiro, A. 263
Chan, K.F. 245
Chan, P.W. 245
Chang, J.F. 319
Chaudhari, S.M. 340
Chen, G. 37
Chen, M.-C. 213
Choi, H.M. 298
Choi, S.K. 298
Choy, C.L. 245
Chuang, J.-C. 213
Cocivera, M. 14

Dandy, D.S. 108
DasGupta, D. 117
Dauscher, A. 132
Dequiedt, A.S. 63
Desu, S.B. 148
Dimigen, H. 206
Dos Santos, M.P. 56
Dultsev, F.N. 303
Dumas, J. 238
Durose, K. 314

Eason, R.W. 259
Eggleston, J.M. 314
Ehara, S. 198
Erçelebi, Ç. 334

Flory, F. 259
Fotakis, C. 259
Fukunaga, N. 6
Futsuhara, M. 274

Gangurde, K.D. 1
Gaze, J. 28
Gazicki, M. 123
Ge, C.-Z. 323
Germi, P. 143
Glass Jr., J.A. 138
Golego, N. 14
Greer, A.L. 46
Grischke, M. 206
Grivas, C. 259
Gudiño-Martínez, A. 282
Gupta, A. 340

Halliday, D.P. 314
He, D. 37
Hirohashi, R. 290
Ho, W. 9
Hsieh, J.C. 98
Hu, X.Z. 225

Ibanez, A. 85
Ichikawa, T. 198
Inoue, Y. 41
Ishigure, K. 188
Izawa, H. 28

Jastrabík, L. 259
Jelínek, M. 259
Jianguo, H. 194
Ju, Y.H. 98
Juodkazis, S. 238

Kapil, R. 74
Karanjai, M.K. 117
Kim, S.P. 298
Komoguchi, T. 41
Kshirsagar, S.T. 167
Kubo, T. 233
Kurokawa, Y. 233
Kwok, R.W.M. 245

Lančok, J. 259
Lawn, B.R. 225
Ledzion, R. 123
Lenoir, B. 132
Li, A.-d. 323
Lin, C. 104
Liu, C.J. 98
Liu, J.-F. 308
Lü, P. 323
Lu, Z.-H. 308

Ma, X. 37
Mahalingam, P. 108

Marathe, B.R. 1
Matazuma, M. 290
Mazurczyk, R. 123
Mehta, B.R. 74
Meng, L.-j. 56
Michler, T. 206
Ming, N.-B. 323
Mingliang, T. 194
Mitra, A. 167
Mohan Rao, K. 340
Mohanty, S. 21
Morales-Acevedo, A. 329
Mostéfa-Sba, H. 63
Mugnier, J. 238
Musale, D.V. 167
Muto, S. 233

Nakata, H. 41
Nanda, K.K. 21
Natarajan, C. 6
Navarro-Contreras, H. 282
Nogami, G. 6

Ong, C.W. 245
Oyanagi, N. 28

Pai, M.P. 167
Parlak, M. 334
Pattabi, M. 340
Pawłowski, S. 123
Pergament, A.L. 33
Pernet, M. 143
Phase, D.M. 340
Philippot, E. 85
Plenet, J.C. 238
Pradhan, A. 74

Ramesham, R. 158
Rashad, A. 1
Ray, S.C. 117
Rigneault, H. 259
Rodrìguez, Y. 329
Rohr, C. 9
Rosendo, E. 282
Roy, C. 74

Sacilotti, M. 63
Sahu, S.N. 21
Sainkar, S.R. 167
Sali, J.V. 1
Sarangi, S.N. 21
Scherrer, H. 132

Senkevich, J.J. 148
Serikawa, T. 198
Shaligram, A.D. 1
Shang, S. 104
Shi, F.F. 254
Shun, T. 194
Shuyuan, Z. 194
Sibillot, P. 63
Somekh, R.E. 46
Spencer, J.T. 138
Stefanovich, G.B. 33
Su, Y.L. 218
Suresh, N. 340
Suzuki, K. 233
Sveshnikova, L.L. 303

Takai, O. 41, 274
Takwale, M.G. 1
Tanaka, T. 290
Tourillon, G. 85
Tourtin, F. 85
Trindade, B. 68
Tsang, Y.C. 245
Tsunooka, M. 198

Uehara, K. 198
Ueng, H.Y. 319

Vaitkus, J.V. 238
Vankar, V.D. 74
Vàzquez-Lòpez, C. 329
Vàzquez-Luna, J.G. 329
Vidal, M.A. 282
Vieira, M.T. 68
Vigil, O. 329

Wang, H. 104
Wang, M. 104
Wang, Z. 104
Watanabe, T. 188
Wei, C.S. 218
Wu, C.T. 218
Wu, D. 323

Xu, C.-Y. 323
Xu, J. 323

Yamamoto, I. 28
Yang, F.-L. 46
Yang, J. 37
Yang, K.-Z. 308
Yao, S.H. 218

PII S0040-6090(98)00831-1

ELSEVIER

Thin Solid Films 322 (1998) 344–345

thin solid films

Author Index of Volume 322

Anderson, A.A. 259
Armand, P. 85
Asai, K. 188

Babelon, P. 63
Banerjee, A. 340
Bellad, S.S. 93
Bernstein, E. 238
Bewilogua, K. 206
Bhosale, C.H. 93
Boffoué, M.O. 132
Boo, J.-H. 9
Bourgeois, S. 63
Bovier, C. 238
Brett, C.M.A. 263
Brunet, F. 143

Carter, G. 177
Cavaleiro, A. 263
Chan, K.F. 245
Chan, P.W. 245
Chang, J.F. 319
Chaudhari, S.M. 340
Chen, G. 37
Chen, M.-C. 213
Choi, H.M. 298
Choi, S.K. 298
Choy, C.L. 245
Chuang, J.-C. 213
Cocivera, M. 14

Dandy, D.S. 108
DasGupta, D. 117
Dauscher, A. 132
Dequiedt, A.S. 63
Desu, S.B. 148
Dimigen, H. 206
Dos Santos, M.P. 56
Dultsev, F.N. 303
Dumas, J. 238
Durose, K. 314

Eason, R.W. 259
Eggleston, J.M. 314
Ehara, S. 198
Erçelebi, Ç. 334

Flory, F. 259
Fotakis, C. 259
Fukunaga, N. 6
Futsuhara, M. 274

Gangurde, K.D. 1
Gaze, J. 28
Gazicki, M. 123
Ge, C.-Z. 323
Germi, P. 143
Glass Jr., J.A. 138
Golego, N. 14
Greer, A.L. 46
Grischke, M. 206
Grivas, C. 259
Gudiño-Martínez, A. 282
Gupta, A. 340

Halliday, D.P. 314
He, D. 37
Hirohashi, R. 290
Ho, W. 9
Hsieh, J.C. 98
Hu, X.Z. 225

Ibanez, A. 85
Ichikawa, T. 198
Inoue, Y. 41
Ishigure, K. 188
Izawa, H. 28

Jastrabík, L. 259
Jelínek, M. 259
Jianguo, H. 194
Ju, Y.H. 98
Juodkazis, S. 238

Kapil, R. 74
Karanjai, M.K. 117
Kim, S.P. 298
Komoguchi, T. 41
Kshirsagar, S.T. 167
Kubo, T. 233
Kurokawa, Y. 233
Kwok, R.W.M. 245

Lančok, J. 259
Lawn, B.R. 225
Ledzion, R. 123
Lenoir, B. 132
Li, A.-d. 323
Lin, C. 104
Liu, C.J. 98
Liu, J.-F. 308
Lü, P. 323
Lu, Z.-H. 308

Ma, X. 37
Mahalingam, P. 108

Marathe, B.R. 1
Matazuma, M. 290
Mazurczyk, R. 123
Mehta, B.R. 74
Meng, L.-j. 56
Michler, T. 206
Ming, N.-B. 323
Mingliang, T. 194
Mitra, A. 167
Mohan Rao, K. 340
Mohanty, S. 21
Morales-Acevedo, A. 329
Mostéfa-Sba, H. 63
Mugnier, J. 238
Musale, D.V. 167
Muto, S. 233

Nakata, H. 41
Nanda, K.K. 21
Natarajan, C. 6
Navarro-Contreras, H. 282
Nogami, G. 6

Ong, C.W. 245
Oyanagi, N. 28

Pai, M.P. 167
Parlak, M. 334
Pattabi, M. 340
Pawłowski, S. 123
Pergament, A.L. 33
Pernet, M. 143
Phase, D.M. 340
Philippot, E. 85
Plenet, J.C. 238
Pradhan, A. 74

Ramesham, R. 158
Rashad, A. 1
Ray, S.C. 117
Rigneault, H. 259
Rodrìguez, Y. 329
Rohr, C. 9
Rosendo, E. 282
Roy, C. 74

Sacilotti, M. 63
Sahu, S.N. 21
Sainkar, S.R. 167
Sali, J.V. 1
Sarangi, S.N. 21
Scherrer, H. 132

Senkevich, J.J. 148
Serikawa, T. 198
Shaligram, A.D. 1
Shang, S. 104
Shi, F.F. 254
Shun, T. 194
Shuyuan, Z. 194
Sibillot, P. 63
Somekh, R.E. 46
Spencer, J.T. 138
Stefanovich, G.B. 33
Su, Y.L. 218
Suresh, N. 340
Suzuki, K. 233
Sveshnikova, L.L. 303

Takai, O. 41, 274
Takwale, M.G. 1
Tanaka, T. 290
Tourillon, G. 85
Tourtin, F. 85
Trindade, B. 68
Tsang, Y.C. 245
Tsunooka, M. 198

Uehara, K. 198
Ueng, H.Y. 319

Vaitkus, J.V. 238
Vankar, V.D. 74
Vàzquez-Lòpez, C. 329
Vàzquez-Luna, J.G. 329
Vidal, M.A. 282
Vieira, M.T. 68
Vigil, O. 329

Wang, H. 104
Wang, M. 104
Wang, Z. 104
Watanabe, T. 188
Wei, C.S. 218
Wu, C.T. 218
Wu, D. 323

Xu, C.-Y. 323
Xu, J. 323

Yamamoto, I. 28
Yang, F.-L. 46
Yang, J. 37
Yang, K.-Z. 308
Yao, S.H. 218

PII S0040-6090(98)00831-1

Yoshikawa, S. 198
Yoshioka, K. 274
Young, T.F. 319
Yu, S. 254
Yuheng, Z. 194
Zelaya-Angel, O. 329
Zeng, J. 104
Zhao, X.-A. 245
Zhiwen, C. 194

ELSEVIER

Thin Solid Films 322 (1998) 346–350

thin solid films

Subject Index of Volume 322

AC impedance
Determination of flatband potential for boron doped diamond electrode in 0.5 M NaCl by AC impedance spectroscopy, 158
Al metallization
A study on the crystallographic orientation with residual stress and electrical property of Al films deposited by sputtering, 298
Aluminium oxide
Third-order nonlinear optical properties of Disperse Red 1 and Au nanometer-size particle-doped alumina films prepared by the sol–gel method, 233
Aluminum corrosion
Redox reaction at the two-layer interface between aluminum and electropolymerized poly(3-methylthiophene) thin solid films, 198
Amorphous materials
Interelectrode separation effects on a-SiGe:H films prepared by plasma chemical vapor deposition, 1
Synthesis of Sn-doped a-C:H films by RF plasma-enhanced chemical vapor deposition and their characterization, 41
Amorphous W–Co–C sputtered films
Crystallisation kinetics of amorphous W–Co–C sputtered films, 68
Annealing
Gallium phosphate thin solid films: structural and chemical determination of the oxygen surroundings by XANES and XPS, 85
Study on annealing effects of Au thin films on Si, 319
Anodic oxidation
Phase composition of anodic oxide films on transition metals: a thermodynamic approach, 33
Atmospheric-pressure metalorganic chemical vapor deposition
Preparation and ferroelectric properties of $BaTiO_3$ thin films by atmospheric-pressure metalorganic chemical vapor deposition, 104
Atomic force microscopy
Langmuir–Blodgett films of poly-*N*-vinylcarbazole prepared by radical polymerization method, 308

Band gap
Modulated photocurrent of evaporated copper phthalocyanine thin films, 290
Bilayer structures
A simple indentation stress–strain relation for contacts with spheres on bilayer structures, 225
Bismuth
Pulsed laser deposition of bismuth in the presence of different ambient atmospheres, 132
c-BN thin film
Temperature effects on growth of boron nitride thin films by a hot filament assisted rf plasma chemical vapor deposition, 37
Boron doped diamond films
Microstructural study of boron doped diamond films by X-ray diffraction profiles analysis, 143
Boron nitride
The growth of hexagonal boron nitride thin films on silicon using single source precursor, 9

Cadmium sulfide
Optical properties of CdS nanocrystalline films prepared by a precipitation technique, 21
Cadmium sulphide
Waveguiding properties of CdS-doped SiO_2–TiO_2 films prepared by sol–gel method, 238
Carbon
Synthesis of Sn-doped a-C:H films by RF plasma-enhanced chemical vapor deposition and their characterization, 41
CdS film
Properties of CdS thin films chemically deposited in the presence of a magnetic field, 329
CdTe/CdS solar cell
A study of the depth dependence of photoluminescence from thin film CdS/CdTe solar cells using bevel etched samples, 314
Chemical bath deposition technique
Properties of CdS thin films chemically deposited in the presence of a magnetic field, 329
Chemical vapor deposition
A quasi-equilibrium model for the prediction of interlayer chemistry during diamond chemical vapor deposition, 108
Chemical vapour deposition (CVD)
The growth of hexagonal boron nitride thin films on silicon using single source precursor, 9
Effect of coupling of radio-frequency plasma on the growth of diamond films in a hot filament reactor, 167
Chromium carbonitride (Cr(C, N))
Evaluation on the tension and fatigue behavior of various PVD coated materials, 218
Chromium nitride (CrN)
Evaluation on the tension and fatigue behavior of various PVD coated materials, 218
Clusters
Waveguiding properties of CdS-doped SiO_2–TiO_2 films prepared by sol–gel method, 238
Coatings
Properties of duplex coatings prepared by plasma nitriding and PVD Ti–C:H deposition on X20Cr13 ferritic stainless steel, 206
Waveguiding pulsed laser deposited Ti:sapphire layers on quartz, 259
Coercive field
Preparation and ferroelectric properties of $BaTiO_3$ thin films by atmospheric-pressure metalorganic chemical vapor deposition, 104
CO_2 laser
Laser ablation doping process for the synthesis of conductive diamond thin film, 28
Conductive diamond
Laser ablation doping process for the synthesis of conductive diamond thin film, 28
Conductivity
Substrate temperature dependent properties of sprayed $CoFe_2O_4$ ferrite thin films, 93
Relationship between the structure and the optical and electrical properties of ion beam deposited CN_x films, 245

PII S0040-6090(98)00832-3

Langmuir–Blodgett films of poly-*N*-vinylcarbazole prepared by radical polymerization method, 308
Copper phthalocyanine
Modulated photocurrent of evaporated copper phthalocyanine thin films, 290
Corrosion
A comparison of the electrochemical behaviour of W–M–N (M = Ni, Ti, Al) thin film coatings on high speed steel, 263
Crystal growth
Pulsed laser deposition of bismuth in the presence of different ambient atmospheres, 132
Crystallisation kinetics
Crystallisation kinetics of amorphous W–Co–C sputtered films, 68
$Cu/SiO_2/Si$
Properties of thin Ta–N films reactively sputtered on $Cu/SiO_2/Si$ substrates, 213
CVD diamond
Determination of flatband potential for boron doped diamond electrode in 0.5 M NaCl by AC impedance spectroscopy, 158

Deposition process
Deposition and characterization of $Zn_xCd_{1-x}S$ thin films prepared by the dip technique, 117
Diamond
Effect of coupling of radio-frequency plasma on the growth of diamond films in a hot filament reactor, 167
Diamond films
A quasi-equilibrium model for the prediction of interlayer chemistry during diamond chemical vapor deposition, 108
Diamond thin films
Growth of diamond thin films in a cyclic growth–etch oxy-acetylene flame process, 74
Dichloro-*t*-butylphosphine
Epitaxial growth with phosphorus. 4. Application of dichloro-*t*-butylphosphine to CVD processes: the thermal chemical vapor deposition formation of copper phosphide thin films and etching of indium phosphide by dichloro-*t*-butylphosphine [1], 138
Differential scanning calorimetry
Crystallisation kinetics of amorphous W–Co–C sputtered films, 68
Dopant anion
Redox reaction at the two-layer interface between aluminum and electropolymerized poly(3-methylthiophene) thin solid films, 198
DUV
Electron beam stabilization and dissolution behaviors of advanced deep UV photoresist for sub 0.3 μm microelectronics fabrication, 254

E-beam
Electron beam stabilization and dissolution behaviors of advanced deep UV photoresist for sub 0.3 μm microelectronics fabrication, 254
Electrical properties
Structural, electrical and optical properties of zinc nitride thin films prepared by reactive rf magnetron sputtering, 274
Electrical properties and measurements
Interelectrode separation effects on a-SiGe:H films prepared by plasma chemical vapor deposition, 1
Electrical resistivity
Substrate temperature dependent properties of sprayed $CoFe_2O_4$ ferrite thin films, 93
Endurance limit (fatigue limit)
Evaluation on the tension and fatigue behavior of various PVD coated materials, 218
Etching
Growth of diamond thin films in a cyclic growth–etch oxy-acetylene flame process, 74

Ferroelectrics
Raman spectroscopy and X-ray diffraction study of sol–gel derived $(Pb_{1-x}La_x)Ti_{1-x/4}O_3$ thin films on Si substrates, 323
Ferroelectric thin film
Preparation and ferroelectric properties of $BaTiO_3$ thin films by atmospheric-pressure metalorganic chemical vapor deposition, 104
Filament temperature
Temperature effects on growth of boron nitride thin films by a hot filament assisted rf plasma chemical vapor deposition, 37
Film deposition
Surface roughening during ion-assisted film deposition, 177
Film deposition technique
The effect of substrate and post-annealing temperature on the structural and optical properties of polycrystalline InSe thin films, 334
Flatband potential
Determination of flatband potential for boron doped diamond electrode in 0.5 M NaCl by AC impedance spectroscopy, 158
Fractal crystallization
Fractal formation and tunnelling effects on the conductivity of Au/a-Ge bilayer films, 194
Fractal dimension
Fractal formation and tunnelling effects on the conductivity of Au/a-Ge bilayer films, 194

Gallium phosphate
Gallium phosphate thin solid films: structural and chemical determination of the oxygen surroundings by XANES and XPS, 85
Gas sensor
Response characteristics of lead phthalocyanine gas sensor: effects of film thickness and crystal morphology, 98
Germanium/carbon films
Deposition and properties of germanium/carbon films deposited from tetramethylgermanium in a parallel plate RF discharge, 123
Glow discharge
Interelectrode separation effects on a-SiGe:H films prepared by plasma chemical vapor deposition, 1
Deposition and properties of germanium/carbon films deposited from tetramethylgermanium in a parallel plate RF discharge, 123
Gold
Third-order nonlinear optical properties of Disperse Red 1 and Au nanometer-size particle-doped alumina films prepared by the sol–gel method, 233
Growth mechanism
Phase composition of anodic oxide films on transition metals: a thermodynamic approach, 33

Hard coatings
A comparison of the electrochemical behaviour of W–M–N (M = Ni, Ti, Al) thin film coatings on high speed steel, 263
Heterostructures
The growth of hexagonal boron nitride thin films on silicon using single source precursor, 9
High speed steel
A comparison of the electrochemical behaviour of W–M–N (M = Ni, Ti, Al) thin film coatings on high speed steel, 263
Hot filament CVD
Temperature effects on growth of boron nitride thin films by a hot filament assisted rf plasma chemical vapor deposition, 37

Indium phosphide
Epitaxial growth with phosphorus. 4. Application of dichloro-*t*-butylphosphine to CVD processes: the thermal chemical vapor deposition formation of copper phosphide thin films and etching of indium phosphide by dichloro-*t*-butylphosphine [1], 138
Indium tin oxide
Properties of indium tin oxide films prepared by rf reactive magnetron sputtering at different substrate temperature, 56

Infrared spectroscopy
Relationship between the structure and the optical and electrical properties of ion beam deposited CN_x films, 245
InP
Luminescence of spark processed porous InP, 282
InSe thin films
The effect of substrate and post-annealing temperature on the structural and optical properties of polycrystalline InSe thin films, 334
Insulator
SEM and XPS studies of titanium dioxide thin films grown by MOCVD, 63
Ion irradiation
Surface roughening during ion-assisted film deposition, 177

J-aggregates
Control of domain structure of a cyanine dye Langmuir–Blodgett film, 188

Langmuir–Blodgett films
Langmuir–Blodgett films of poly-*N*-vinylcarbazole prepared by radical polymerization method, 308
Langmuir–Blodgett layers
Determination of structure and shape of nanoclusters obtained in sulphidation of Langmuir–Blodgett layers, 303
Laser ablation
Waveguiding pulsed laser deposited Ti:sapphire layers on quartz, 259
LB films
Control of domain structure of a cyanine dye Langmuir–Blodgett film, 188
Lead phthalocyanine
Response characteristics of lead phthalocyanine gas sensor: effects of film thickness and crystal morphology, 98
Line profile
Microstructural study of boron doped diamond films by X-ray diffraction profiles analysis, 143
Lithium ion battery
Titanium dioxide thin film deposited by spray pyrolysis of aqueous solution, 6
Luminescence
Optical properties of CdS nanocrystalline films prepared by a precipitation technique, 21
Waveguiding pulsed laser deposited Ti:sapphire layers on quartz, 259

Magnetic field
Properties of CdS thin films chemically deposited in the presence of a magnetic field, 329
Magnetron sputtering
Properties of indium tin oxide films prepared by rf reactive magnetron sputtering at different substrate temperature, 56
Microelectronics
Electron beam stabilization and dissolution behaviors of advanced deep UV photoresist for sub 0.3 μm microelectronics fabrication, 254
MOCVD
SEM and XPS studies of titanium dioxide thin films grown by MOCVD, 63
Modulated photocurrent
Modulated photocurrent of evaporated copper phthalocyanine thin films, 290
Mott–Schottky plot
Determination of flatband potential for boron doped diamond electrode in 0.5 M NaCl by AC impedance spectroscopy, 158

Nanoclusters
Determination of structure and shape of nanoclusters obtained in sulphidation of Langmuir–Blodgett layers, 303
Nanostructures
Optical properties of CdS nanocrystalline films prepared by a precipitation technique, 21
Nitride
Structural, electrical and optical properties of zinc nitride thin films prepared by reactive rf magnetron sputtering, 274
Nonlinear conductivity
Study on annealing effects of Au thin films on Si, 319

Optical properties
Optical properties of CdS nanocrystalline films prepared by a precipitation technique, 21
Deposition and characterization of $Zn_xCd_{1-x}S$ thin films prepared by the dip technique, 117
Waveguiding properties of CdS-doped SiO_2–TiO_2 films prepared by sol–gel method, 238
Structural, electrical and optical properties of zinc nitride thin films prepared by reactive rf magnetron sputtering, 274
Organometallic vapour deposition
The growth of hexagonal boron nitride thin films on silicon using single source precursor, 9
Deposition and properties of germanium/carbon films deposited from tetramethylgermanium in a parallel plate RF discharge, 123
Orientation
A study on the crystallographic orientation with residual stress and electrical property of Al films deposited by sputtering, 298
Oxides
Phase composition of anodic oxide films on transition metals: a thermodynamic approach, 33
SEM and XPS studies of titanium dioxide thin films grown by MOCVD, 63
Oxy-acetylene flame process
Growth of diamond thin films in a cyclic growth–etch oxy-acetylene flame process, 74

Phase shift
Modulated photocurrent of evaporated copper phthalocyanine thin films, 290
Photolithography
Electron beam stabilization and dissolution behaviors of advanced deep UV photoresist for sub 0.3 μm microelectronics fabrication, 254
Photoluminescence
Luminescence of spark processed porous InP, 282
A study of the depth dependence of photoluminescence from thin film CdS/CdTe solar cells using bevel etched samples, 314
Photoresist
Electron beam stabilization and dissolution behaviors of advanced deep UV photoresist for sub 0.3 μm microelectronics fabrication, 254
Photovoltage
Optical properties of CdS nanocrystalline films prepared by a precipitation technique, 21
Plasma nitriding
Properties of duplex coatings prepared by plasma nitriding and PVD Ti–C:H deposition on X20Cr13 ferritic stainless steel, 206
Plasma processing and deposition
Synthesis of Sn-doped a-C:H films by RF plasma-enhanced chemical vapor deposition and their characterization, 41
PLT
Raman spectroscopy and X-ray diffraction study of sol–gel derived $(Pb_{1-x}La_x)Ti_{1-x/4}O_3$ thin films on Si substrates, 323
Poly(chloro-*p*-xylylene)
Poly(chloro-*p*-xylylene)/SiO_2 multilayer thin films deposited near-room temperature by thermal CVD, 148
Polymer
Poly(chloro-*p*-xylylene)/SiO_2 multilayer thin films deposited near-room temperature by thermal CVD, 148

Poly(3-methyl thiophene)
Redox reaction at the two-layer interface between aluminum and electropolymerized poly(3-methylthiophene) thin solid films, 198
Poly-*N*-vinylcarbazole
Langmuir–Blodgett films of poly-*N*-vinylcarbazole prepared by radical polymerization method, 308
Post-annealing temperature
The effect of substrate and post-annealing temperature on the structural and optical properties of polycrystalline InSe thin films, 334
Potassium titanyl phosphate
Polycrystalline $RbTiOPO_4$ and $KTiOPO_4$ bilayer thin films by spray pyrolysis, 14
Pulsed laser deposition
Pulsed laser deposition of bismuth in the presence of different ambient atmospheres, 132
Pyrosol
Gallium phosphate thin solid films: structural and chemical determination of the oxygen surroundings by XANES and XPS, 85

Quasi-equilibrium model
A quasi-equilibrium model for the prediction of interlayer chemistry during diamond chemical vapor deposition, 108

Raman scattering
Effect of coupling of radio-frequency plasma on the growth of diamond films in a hot filament reactor, 167
Raman spectroscopy
Raman spectroscopy and X-ray diffraction study of sol–gel derived $(Pb_{1-x}La_x)Ti_{1-x/4}O_3$ thin films on Si substrates, 323
Random Tunnelling Junction Network (RTJN) model
Fractal formation and tunnelling effects on the conductivity of Au/a-Ge bilayer films, 194
Rapid thermal annealing
Preparation and ferroelectric properties of $BaTiO_3$ thin films by atmospheric-pressure metalorganic chemical vapor deposition, 104
Redox reaction
Redox reaction at the two-layer interface between aluminum and electropolymerized poly(3-methylthiophene) thin solid films, 198
Remanent polarization
Preparation and ferroelectric properties of $BaTiO_3$ thin films by atmospheric-pressure metalorganic chemical vapor deposition, 104
Residual stress
A study on the crystallographic orientation with residual stress and electrical property of Al films deposited by sputtering, 298
Resistance
Fractal formation and tunnelling effects on the conductivity of Au/a-Ge bilayer films, 194
Resistivity
A study on the crystallographic orientation with residual stress and electrical property of Al films deposited by sputtering, 298
Response time
Response characteristics of lead phthalocyanine gas sensor: effects of film thickness and crystal morphology, 98
Rubidium titanyl phosphate
Polycrystalline $RbTiOPO_4$ and $KTiOPO_4$ bilayer thin films by spray pyrolysis, 14

Scanning electron microscopy
Pulsed laser deposition of bismuth in the presence of different ambient atmospheres, 132
SEM
Redox reaction at the two-layer interface between aluminum and electropolymerized poly(3-methylthiophene) thin solid films, 198
Silicon dioxide
Poly(chloro-*p*-xylylene)/SiO_2 multilayer thin films deposited near-room temperature by thermal CVD, 148
Silicon substrates
Gallium phosphate thin solid films: structural and chemical determination of the oxygen surroundings by XANES and XPS, 85
Slow discharge
Effect of coupling of radio-frequency plasma on the growth of diamond films in a hot filament reactor, 167
Sol–gel
Raman spectroscopy and X-ray diffraction study of sol–gel derived $(Pb_{1-x}La_x)Ti_{1-x/4}O_3$ thin films on Si substrates, 323
Sol–gel method
Third-order nonlinear optical properties of Disperse Red 1 and Au nanometer-size particle-doped alumina films prepared by the sol–gel method, 233
Solid boron
Laser ablation doping process for the synthesis of conductive diamond thin film, 28
Spark-processed
Luminescence of spark processed porous InP, 282
Spectra
Redox reaction at the two-layer interface between aluminum and electropolymerized poly(3-methylthiophene) thin solid films, 198
Spheres
A simple indentation stress–strain relation for contacts with spheres on bilayer structures, 225
Spray pyrolysis
Polycrystalline $RbTiOPO_4$ and $KTiOPO_4$ bilayer thin films by spray pyrolysis, 14
Spreading–compression method
Control of domain structure of a cyanine dye Langmuir–Blodgett film, 188
Sputtering
Relationship between the structure and the optical and electrical properties of ion beam deposited CN_x films, 245
Structural, electrical and optical properties of zinc nitride thin films prepared by reactive rf magnetron sputtering, 274
Steel
Properties of duplex coatings prepared by plasma nitriding and PVD Ti–C:H deposition on X20Cr13 ferritic stainless steel, 206
Stress–strain relation
A simple indentation stress–strain relation for contacts with spheres on bilayer structures, 225
Structural properties
Structural, electrical and optical properties of zinc nitride thin films prepared by reactive rf magnetron sputtering, 274
Substrate–temperature
UHV magnetron sputtering of silver films on rocksalt: quantitative X-ray texture analysis of substrate-temperature-dependent microstructure, 46
Substrate temperature
Properties of indium tin oxide films prepared by rf reactive magnetron sputtering at different substrate temperature, 56
The effect of substrate and post-annealing temperature on the structural and optical properties of polycrystalline InSe thin films, 334
Sulphidation
Determination of structure and shape of nanoclusters obtained in sulphidation of Langmuir–Blodgett layers, 303
Surface morphology
Deposition and characterization of $Zn_xCd_{1-x}S$ thin films prepared by the dip technique, 117
Surface roughening
Surface roughening during ion-assisted film deposition, 177

Ta–N
Properties of thin Ta–N films reactively sputtered on Cu/SiO_2/Si substrates, 213

Temperature
Substrate temperature dependent properties of sprayed $CoFe_2O_4$ ferrite thin films, 93
Aging studies on discontinuous silver films in ultrahigh vacuum, 340
Tensile stress
Preparation and ferroelectric properties of $BaTiO_3$ thin films by atmospheric-pressure metalorganic chemical vapor deposition, 104
Tetramethylgermanium
Deposition and properties of germanium/carbon films deposited from tetramethylgermanium in a parallel plate RF discharge, 123
Thin film
Titanium dioxide thin film deposited by spray pyrolysis of aqueous solution, 6
Study on annealing effects of Au thin films on Si, 319
Thin film properties
Properties of thin Ta–N films reactively sputtered on $Cu/SiO_2/Si$ substrates, 213
Thin films
A comparison of the electrochemical behaviour of W–M–N (M = Ni, Ti, Al) thin film coatings on high speed steel, 263
Third-order nonlinear optics
Third-order nonlinear optical properties of Disperse Red 1 and Au nanometer-size particle-doped alumina films prepared by the sol–gel method, 233
TiO_2
SEM and XPS studies of titanium dioxide thin films grown by MOCVD, 63
Titanium carbonitride (Ti(C, N))
Evaluation on the tension and fatigue behavior of various PVD coated materials, 218
Titanium dioxide
Titanium dioxide thin film deposited by spray pyrolysis of aqueous solution, 6
Titanium nitride (TiN)
Evaluation on the tension and fatigue behavior of various PVD coated materials, 218
Titanium oxide
SEM and XPS studies of titanium dioxide thin films grown by MOCVD, 63
Waveguiding pulsed laser deposited Ti:sapphire layers on quartz, 259
Transition
Aging studies on discontinuous silver films in ultrahigh vacuum, 340
Trimethylindium
Epitaxial growth with phosphorus. 4. Application of dichloro-*t*-butylphosphine to CVD processes: the thermal chemical vapor deposition formation of copper phosphide thin films and etching of indium phosphide by dichloro-*t*-butylphosphine [**1**], 138
Tungsten-based coatings
A comparison of the electrochemical behaviour of W–M–N (M = Ni, Ti, Al) thin film coatings on high speed steel, 263

UHV magnetron
UHV magnetron sputtering of silver films on rocksalt: quantitative X-ray texture analysis of substrate-temperature-dependent microstructure, 46
Ultrathin films
Poly(chloro-*p*-xylylene)/SiO_2 multilayer thin films deposited near-room temperature by thermal CVD, 148

Vacuum
Aging studies on discontinuous silver films in ultrahigh vacuum, 340

X-ray photoelectron spectroscopy (XPS)
Relationship between the structure and the optical and electrical properties of ion beam deposited CN_x films, 245
X-ray diffraction
UHV magnetron sputtering of silver films on rocksalt: quantitative X-ray texture analysis of substrate-temperature-dependent microstructure, 46
Crystallisation kinetics of amorphous W–Co–C sputtered films, 68
Deposition and characterization of $Zn_xCd_{1-x}S$ thin films prepared by the dip technique, 117
X-ray diffraction pattern
Microstructural study of boron doped diamond films by X-ray diffraction profiles analysis, 143
X-ray photoelectron spectroscopy
Synthesis of Sn-doped a-C:H films by RF plasma-enhanced chemical vapor deposition and their characterization, 41
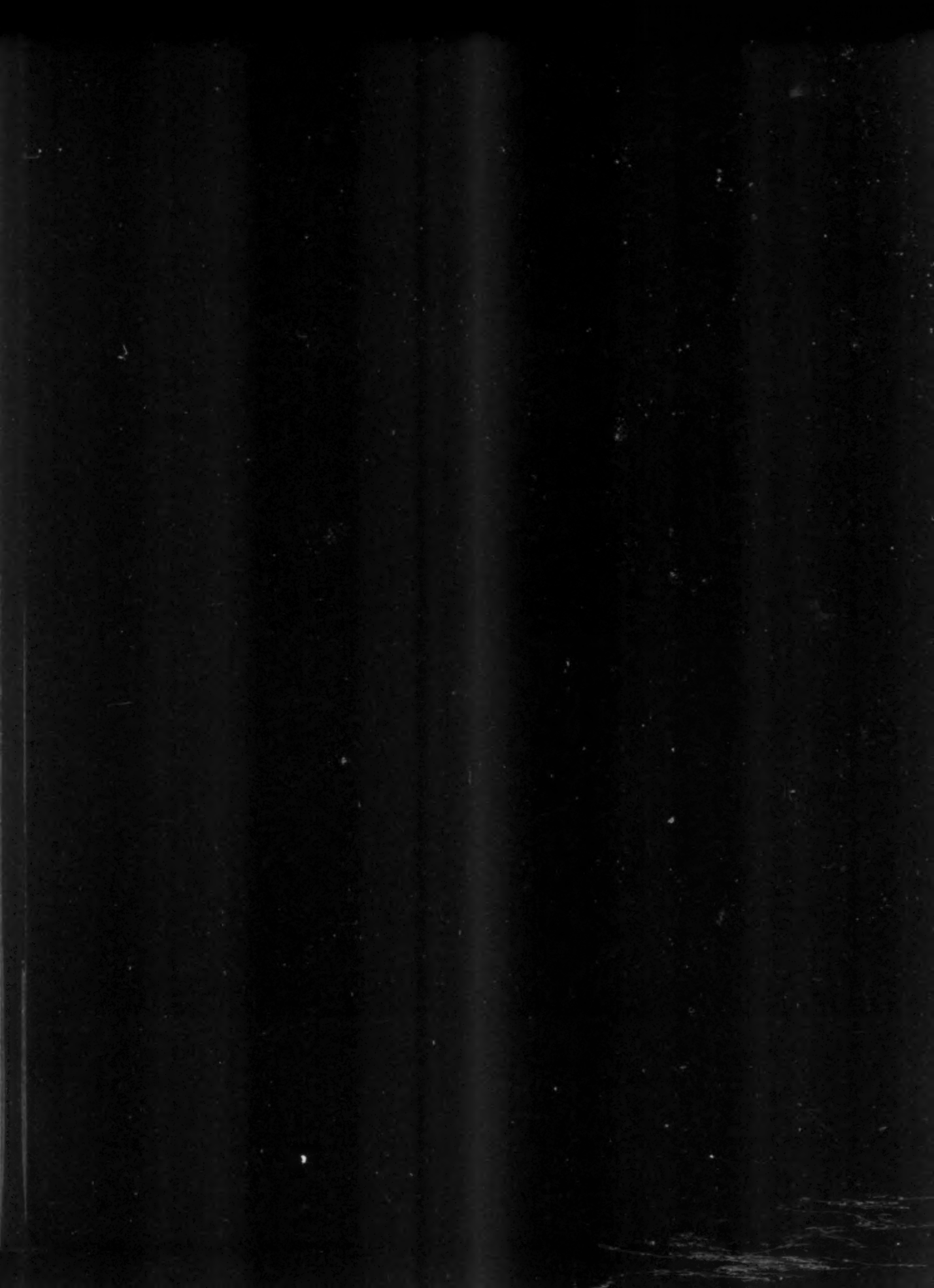
Zinc
Structural, electrical and optical properties of zinc nitride thin films prepared by reactive rf magnetron sputtering, 274